Sensors and Actuators B 251 (2017) 57–64

Contents lists available at ScienceDirect

Sensors and Actuators B: Chemical

journal homepage: www.elsevier.com/locate/snb

Research Paper

Hydrogen sensors based on 2D WO_3 nanosheets prepared by anodization

Mohammad Bagher Rahmani[a,*], Mohd Hanif Yaacob[b], Ylias Mohammad Sabri[c]

[a] Department of Physics, Shahrood University of Technology, Shahrood, Semnan 3619995161, Iran
[b] Wireless and Photonic Network Research Centre, Faculty of Engineering, Universiti Putra Malaysia, 43400 UPM Serdang, Selangor, Malaysia
[c] Centre for Advanced Materials and Industrial Chemistry (CAMIC), School of Science, RMIT University, Melbourne, Victoria 3001, Australia

ARTICLE INFO

Article history:
Received 30 October 2016
Received in revised form 24 April 2017
Accepted 8 May 2017
Available online 10 May 2017

Keywords:
Hydrogen
2D nanostructures
Gas sensing
Anodization
Tungsten trioxide
Surface properties

ABSTRACT

Two dimensional tungsten trioxide (WO_3) films made of nanosheets were prepared using high temperature anodization of tungsten (W) thin films. The W thin films were deposited by R.F. magnetron sputtering onto quartz substrates and then anodized at 50 °C in an aqueous solution containing 1.5 M HNO_3. The structural and morphological properties of the prepared films were fully characterized prior to employing them for hydrogen gas sensing application. The hydrogen gas sensing performance of WO_3 thin films was investigated at different temperatures through the measurement of conductance changes upon gas exposure. Hydrogen gas exposure resulted in the intercalation and subsequent reduction of WO_3 sheets, changing the charge carrier concentration and hence the conductivity of the films. The fabricated sensors were found to exhibit excellent sensitivity and repeatability when they were exposed to hydrogen gas while using air as the carrier gas. The effects of different operating temperatures on the sensitivity of the devices were studied in the range of 20–250 °C. The dynamic response of the 2D WO_3 nanosheets based sensors at different operating temperatures are presented and discussed.

1. Introduction

Gas sensing devices are becoming increasingly mandatory for industrial health and safety requirements, as well as for environmental monitoring, explosives detection, automotive applications and manufacturing process control. To meet these demands, the sensitivity, selectivity and stability of gas sensors need to be significantly improved to exceed the required standards [1–3]. The selection of optimal sensing material is an important problem in both design and fabrication of gas sensor with required operation parameters (such as adsorption and desorption ability; electronic and chemical properties; thermodynamic stability; crystal structure; compatibility with gas sensors fabrication processes). Various gas sensor's devices based on semiconducting metal oxides, covalent semiconductors, solid-state electrolytes, polymers, etc. have been fabricated [4]. For example, polyaniline (PANI), as a type of polymer, has found to be a good gas sensing material for NH_3 because of its simple synthesis, low cost monomer, low toxicity, high response and room temperature sensing. However, PANI shows a low baseline stability in response to NH_3 [5]. In general, polymers are sensitive to ultra violet (UV) radiation and presence of oxidizing gases and because of either polymerization or destruction, their properties irreversibly change during pretty short term [4]. Conductometric gas sensor devices based on semiconducting metal oxide thin films are the most promising among other types of chemical sensors. This is because of the device small dimensions, low production cost, low power consumption, online operation, and high compatibility with microelectronic fabrication processes [1,6]. Furthermore, recent advances in the synthesis of two dimensional (2D) nanostructured metal oxides in the configurations of nanowires, nanorods, nanobelts, and nano-platelets, have provided the opportunity to greatly enhance the performance of fabricated devices [7–14]. 2D materials can show unique electronic and optical properties when the number of dimensions are reduced, due to changes in the electronic band structure [13]. Recently, fabrication of biosensors and high-performance field effect transistors have been reported using 2D nature of α-MoO_3 [12–14]. These materials can be incorporated as semiconducting gas sensors [12,15]. The performance of such sensors is directly associated with granularity, crystallinity, porosity and surface area-to-volume ratio in the sensitive component [10,16–20]. In general, the sensitivity of semiconductor metal oxide gas sensors increases by decreasing grain sizes to the dimensions which are comparable to the Debye length

* Corresponding author.
E-mail addresses: mbrahmani@shahroodut.ac.ir, mbrahmani@yahoo.com (M.B. Rahmani).

http://dx.doi.org/10.1016/j.snb.2017.05.029
0925-4005/

while providing enough spacing between the grains to allow facile diffusion of the gas species, so that entire thickness of the sensitive layer can be affected by the interactions with the gas molecules [1]. The sensitivity is also affected by the alteration of the electronic structure, which is strongly influenced by the quantum size effects with decreasing particle size [1,21,22]. 2D nanostructures of semiconductor metal oxides, specifically ultrathin nanosheets, possess pronounced quantum surface effects and significant changes in electronic structures and thus in the physical and chemical properties, which is inspiring many fundamental and technological research to be undertaken. Such nanosheets are expected to bridge the gap between the quantum world of zero- or one-dimensional nanomaterials and three-dimensional macroscale bulk materials [8].

Semiconductor metal oxide thin films also offer low cost, reliable performance and easy fabrication using existing planar technologies while maintaining precise control of the film properties [9,22,23]. Among the semiconductor metal oxides, tungsten trioxide (WO_3) nanostructured (including nanorods, nanowires, and nanoplates) thin films can be synthesized to have high surface-to-volume ratio, special electrical properties (due to the effect of quantum confinment on carrier transport phenomena) and excellent gas-sensing properties [24]. Several methods have been used to synthesize tungsten trioxide films in nanostructured forms, including chemical vapour deposition (CVD) [25], thermal evaporation [26], RF sputtering [18,27–29], pulsed laser deposition [30], hydrothermal [24,31] and sol-gel [32,33] techniques. Fast and inexpensive liquid synthesis methods such as anodization and high temperature acid etching have also been shown to give nanostructured WO_3 [18,34,35]. Anodization in fluoride containing electrolyte results in meso/nano tubular or porous films [36], while high temperature etching results in nano-platelet surfaces [35]. The surface morphology of the nanostructured WO_3 prepared via anodization methods can be altered by changing the anodization potential, duration and electrolyte concentration, or by varying the etching temperature and electrolyte ionic type and concentration [18,34,36,37].

Tungsten trioxide is a wide bandgap *n*-type semiconductor metal oxide and has been extensively investigated as a sensing material to detect several gas species such as H_2 [28,38], NH_3 [39,40], H_2S [24,41], NO_x [26,27], O_3 [29] and volatile organic compounds (VOCs) including ethanol and methanol [15,31,42]. Among the gas species, hydrogen (H_2) is a clean, portable and potentially unlimited energy source, with the potential to become a remedy for clean energy generation. However, it has the risk of explosion when the concentration reaches above 4%, requiring only low ignition energy (0.02 mJ) and having large flame propagation velocity in such an event. Due to its molecular size, confinement and containment of this gas is difficult [28]. Therefore, sensing hydrogen is necessary from a safety perspective as well as for combustion control, industrial process control and in medical applications where the presence of hydrogen can indicate certain types of bacterial infection [43]. Additionally, several reports have demonstrated that long exposure to H_2 can cause harmful disorders. For example, the results of histopathologic tissue examination, biological blood studies and bone scintigraphies confirm the non-irreversible toxicity effect of hydrogen after long exposure times (42 days) [44]. According to MSDS No. 1009 (revision 1994), exposure to moderate concentrations of H_2 may cause dizziness, headache, nausea and unconsciousness, due to the reduction of oxygen content in the environment. Exposure to atmospheres containing 8–10% or less oxygen will quickly bring about unconsciousness without warning leaving individuals unable to protect themselves. Lack of sufficient oxygen may cause serious injury or death.

The interaction of WO_3 with the hydrogen atom containing molecules is generally the most efficient when it is of an intercalating nature. In this case, the intercalated H^+ ions are embedded into the crystal structure of WO_3 and the released electrons are transferred to the lowest-lying unoccupied energy levels of WO_3. Such an interaction changes the band structure of the WO_3 system and increases its conductivity, both of which can be used for sensing applications of the hydrogen atom containing molecules [7].

In this report, high temperature anodization technique was employed to synthesize WO_3 nanosheet layers onto quartz substrates to develop conductometric sensors. Morphological and structural characterization of these films were performed using field emission scanning electron microscopy (FESEM), high resolution transmission electron microscopy (HRTEM) and X-ray diffraction (XRD) analysis. Finally, the sensor response toward different H_2 gas concentrations was investigated.

2. Experimental

Quartz substrates were cut into 20 mm × 10 mm pieces and cleaned with acetone, isopropanol (IPA) and DI water before deposition. Tungsten thin films were deposited using a planar R.F. magnetron sputterer. A tungsten metal target of 99.99 % purity was employed. Prior to the deposition, the sputtering chamber was first evacuated to 10^{-5} torr. Thereon argon was introduced into the chamber to increase the pressure to 2×10^{-2} torr prior to the deposition being conducted. The samples' temperatures were elevated to 300 °C and placed 6.5 cm away from the target. The deposition process was performed using a sputtering power of 100 W for a duration of 20 min. The deposited film thicknesses were determined to be approximately 550 nm using a profilometer (Ambios-Technology XP-2). Anodization of the tungsten thin film was performed using a conventional anode (tungsten thin film) – cathode (platinum plate) system, where a 60 V DC potential was applied for a period of 6 h. The process was carried out using an electrolyte medium containing 50 mL of 1.5 M HNO_3 solution. The electrolyte solution was kept at a constant elevated temperature of 50 °C during the process. Anodization current was recorded using a computer with data logger software. After anodization, samples were washed with DI water and dried in a stream of N_2. Samples were annealed at 450 °C in 90% O_2, 10% Ar environment with a constant gas flow rate of approximately 200 sccm, in order to ensure the removal of water molecules from the prepared thin films. Annealing was carried out for 5 h and the temperature was increased slowly at the rate of 2 °C/min and cooled at the same rate after the procedure.

FESEM characterization was carried out using a FEI Nova NanoSEM. High resolution TEM (HRTEM) characterization was carried out using a JEOL JEM 2010 Electron Microscope. Samples for HRTEM were prepared by scraping off the films in ethanol, and subsequently drop casting the solution onto a carbon supported copper TEM grid followed by a slow air-drying procedure. X-ray diffraction (XRD) pattern analysis was carried out using a Bruker D8 Discover micro diffractometer fitted with a GADDS (General Area Detector Diffraction System). Data was collected at room temperature when applying CuKα radiation (λ = 1.54178 Å) with a potential of 40 kV and a current of 40 mA, and filtered with a graphite monochromator in the parallel mode (175 mm collimator with 0.5 mm pinholes).

For the fabrication of conductometric sensors, the sensing area was covered with a physical shadow mask and subsequently a layer of gold with the thickness of 100 nm was sputtered using Gatan PEC™ sputter coating system to form the contact pads. Fabricated Au electrodes had simple pattern and were composed of two parallel pads with the contact pad width of about 2 mm and the length of about 10 mm, so that the active sensing area was about $5 \times 10\ mm^2$. Afterwards, two gold wires were bonded to the gold pads using silver epoxy.

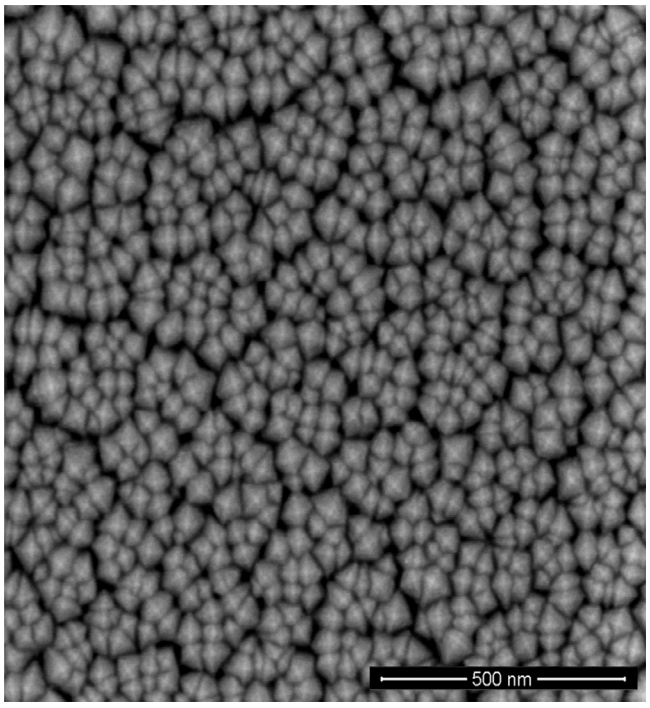

Fig. 1. FESEM micrographs of RF sputtered tungsten thin film surface.

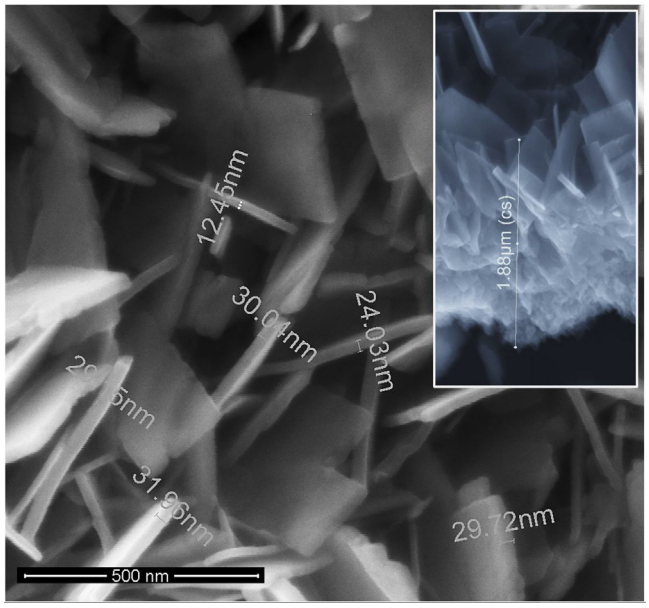

Fig. 2. FESEM micrographs of WO_3 thin film surface (inset shows cross sectional FESEM (45° rotation) of WO_3 film).

For gas sensing measurements, the WO_3 conductometric sensors were mounted on a heater. The measurements were performed in a test chamber made from Teflon, which was sealed using a quartz lid. The heater was controlled by a regulated DC power supply to provide different operating temperatures. The output resistance as a function of time across the conductometric sensor during gas exposure was measured using a multimeter (Keithley 2001). A computerized gas calibration system, with mass flow controllers, was used for exposing the sensor to different concentrations of H_2. The total flow rate was kept constant at 200 sccm and dry synthetic air was used both as the reference and the carrier gas. The test chamber pressure was kept constant at room atmospheric pressure using the exhaust tube for the incoming gas mixture. At each operating temperature, the baseline gas was maintained for a period of 120 min to allow the device to stabilize. Then, the device was exposed to sequences of different concentrations of H_2 for several hours. The sensor temperature was varied in the range of 20–250 °C. Each sequence consisted of exposure to 0.06 (600 ppm), 0.125, 0.25, 0.5 and 1% of H_2 gas balanced in synthetic air. A second pulse of 0.125% H_2 was utilized to confirm the sensors' repeatability. The H_2 and synthetic air exposure times were 10 and 15 min, respectively.

3. Results and discussion

3.1. Thin film characterisation results

Fig. 1 shows the FESEM image of the sputtered tungsten thin film on a quartz substrate. As it can be observed, the sputtered tungsten thin film consists of compact and homogeneous nano-textured grains with the estimated dimensions of less than 100 nm. This is a common morphology that can be observed for tungsten films deposited by RF sputtering process [18].

Following the anodization process, a completely different morphology had appeared as hydrated WO_3 platelets were formed. Annealing at 450 °C for 5 h ensured the removal of the H_2O molecules, where it can be seen in Fig. 2 that the final thin film consisted of vertically standing nano-crystallites with square and rectangular-shaped 2D nanosheets (nano-plateles). The width and the thickness of these 2D nanosheets are in the range of 50–500 nm and 10–50 nm, respectively. From cross-sectional (45° rotation) FESEM image of the sample (inset of Fig. 2), the total thickness of the WO_3 thin film was estimated to be approximately 2 μm. Since gas sensing properties of a metal oxide thin film strongly depends on its morphological features, the observed high surface area facilitates the physisorption and chemisorption processes by increasing the absorption rates. In order to examine the stability of WO_3 nanosheets, FESEM imaging were performed after performing final gas tests, but no changes were observed in the surface morphology of WO_3 nanosheets after gas tests. This is because we annealed samples at 450 °C for 5 h before using as a gas sensor. The mentioned temperature was higher than the optimum working temperature (250 °C) of the fabricated sensor.

The crystal structure of the sample prepared with anodization was determined by XRD. Fig. 3 shows the XRD pattern of the WO_3 thin film measured at room temperature. Three large diffraction peaks of the sample appear at 23.35, 23.75 and 24.4°. Tungsten oxides exhibit many crystal modulations and display characteristic XRD profiles corresponding to different crystal structures [45]. The monoclinic structure characteristically shows three large peaks in the 22–25 ° region correspond to the pseudo-cubic reflections originating from the slight distortion of the ideal cubic (1 0 0) lattice planes [42]. The peak profile is also more complicated than that of the cubic and tetragonal WO_3 crystal structures, but is similar to that of the triclinic and orthorhombic structures [45]. By comparing the XRD pattern with JCPDS cards, best fit were obtained when the peaks were indexed to monoclinic crystal structure with lattice parameters of $a = 7.274$ Å, $b = 7.501$ Å, $c = 3.824$ Å and $\beta = 89.930°$ (JCPDS Card No. 75-2072). Inset in Fig. 3 shows the XRD pattern of as-sputtered tungsten film. Peaks were indexed to cubic crystal structure with lattice parameters of $a = 5.05$ Å, (JCPDS Card No. 47-1319). No tungsten peak can be observed in the WO_3 diffraction pattern, which means that W thin film has been completely oxidized by anodization and annealing processes.

A typical TEM image of the WO_3 nanosheets is depicted in Fig. 4 (a) with the corresponding selected area electron diffraction pattern (SAED) recorded on the thin area. The SAED pattern (the inset in Fig. 4 (a)) was recorded perpendicular to the growth direction of

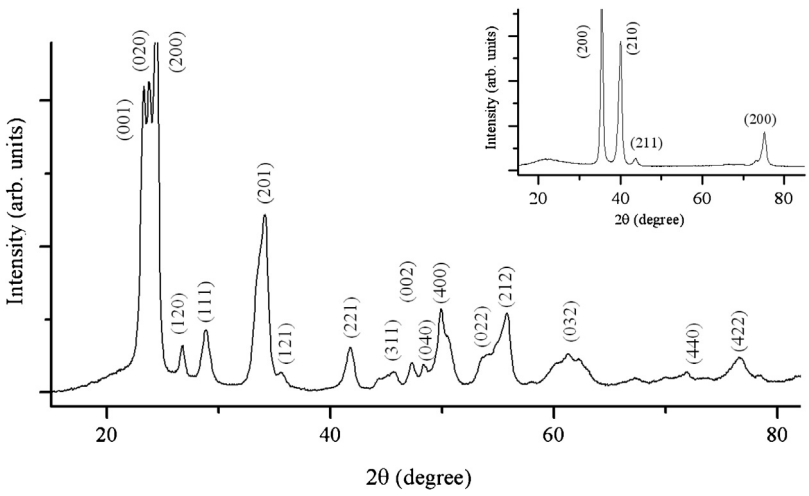

Fig. 3. XRD pattern of WO_3 film (inset shows XRD pattern of sputtered tungsten film).

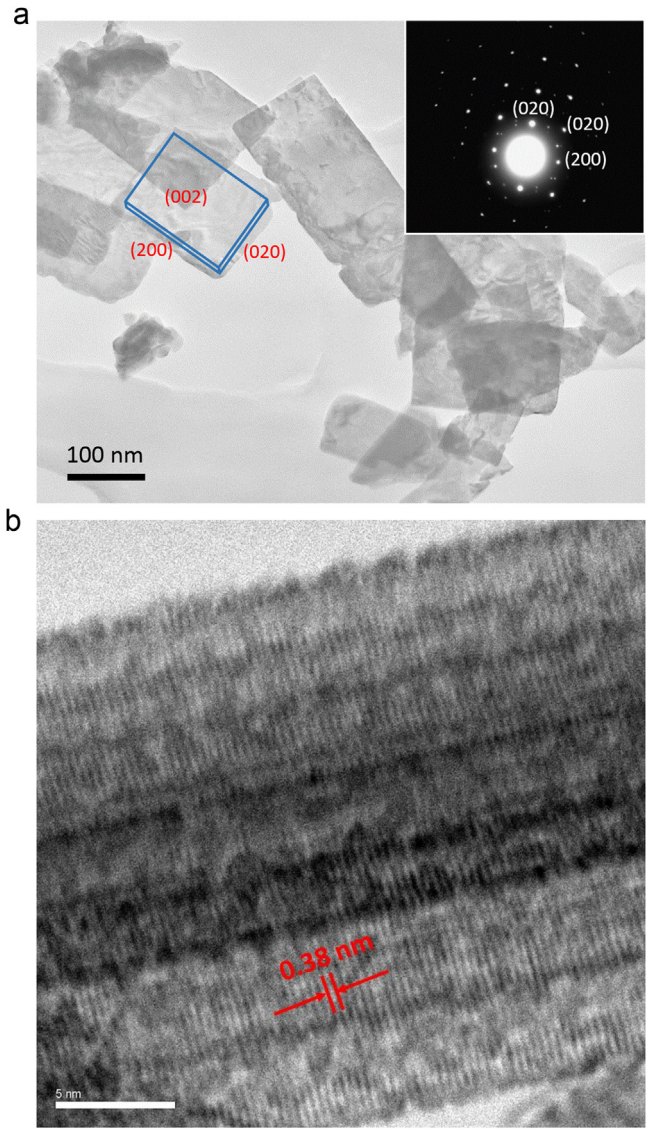

Fig. 4. (a) TEM image of WO_3 nano-platelets (inset shows SAED pattern recorded from a thin area) and (b) HRTEM image of a nano-platelet with estimated lattice spacing.

one single plate. The inset in Fig. 4 (a) presents the corresponding electron diffraction pattern of WO_3 plates, thus indicating the high extent of crystallinity of WO_3. The uniform and ordered diffraction spots can be attributed to the [001] zone axis diffraction of single-crystal monoclinic WO_3, which is also consistent with the XRD results. The recorded image reveals that the surface of rectangular WO_3 nano-platelets consists of a major top (0 0 2), and minor lateral (0 2 0) and (2 0 0) [46]. Fig. 4 (b) shows the HRTEM image of the WO_3 thin film with lattice fringes corresponding to the monoclinic structure. Here, the lattice spacing has been estimated to be about 3.8 Å associated with the (0 0 2) plane of WO_3, which is in consistent with the results reported by others [8,31]. Depending on the synthesis process and annealing temperatures, WO_3 can have different phases such as monoclinic, orthorhombic and tetragonal [33,35]. The crystallographic distortions and tilting of the WO_6 octahedra are responsible for the phase transitions and significantly affect the electronic properties and hence, the device applications of WO_3. It is well-known that WO_3 converts to monoclinic phase at annealing temperatures above 400 °C, which confirms our XRD and SAED results [47].

3.2. Gas sensing results

The developed sensor was tested in a temperature range between 25 to 250 °C. The optimum operating temperature for the sensor response towards H_2 was found to be 250 °C. The curves in Fig. 5. (a) and (b) show dynamic response of the WO_3 sensor towards different concentrations of H_2 gas at 250 °C, first run and second run of gas testing sequences, respectively. 250 °C. Upon the exposure to H_2 gas, the conductivity was increased. If R_{gas} and R_{air} denote the resistance of the sensor in the presence of gas and air, respectively, then the response factor in percentage was defined as $S = (R_{gas} - R_{air} \times 100/R_{air}$. In our case, gas-sensing experiments were performed in dry air atmosphere to avoid any interference from humidity. Exposure to H2 caused a decrease in the resistivity for the WO3 film, indicating *n*-type conduction of the sample.

The gas sensing mechanism is based on the changes in the electrical conductance of the semiconducting oxide film. The electrical conductance of films depends on the content of oxygen ions, oxygen vacancies and the interstitial ions. The oxygen adsorbed depends on the particle size, large specific area of the material, and the operating temperature of the sensor. The oxygen species capture electrons from the material, leading to the increase of the hole concentrations and decrease of the electron concentrations. This reaction takes

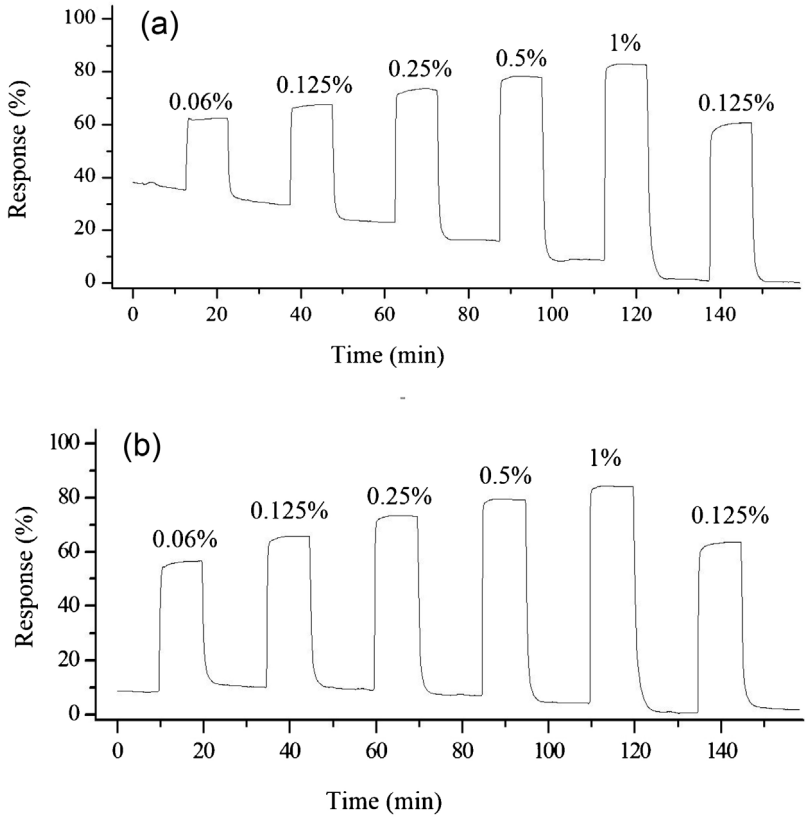

Fig. 5. (a) and (b) Dynamic response of the WO_3 sensor towards different concentrations of H_2 gas at 250 °C, first run and second run of gas testing, respectively.

place prior to sensing and creates a thin electron-depleted layer at the surfaces of the WO_3 grains [48].

When the temperature rises on the walls of 2D WO_3 nanoplatelets, hydrogen molecules start to undergo chemisorption before dissociating into hydrogen ions (H^+) by injecting an electron into the film, according to the following equation [7,49]:

$$H_{2(gas)} \rightarrow 2H^+ + 2e^- \quad (1)$$

The accumulated H^+ ions then diffuse over the surface and intercalate with the WO_3 thin films, the process of which can be described according to the following formula [7,28]:

$$WO_3 + xH^+ + xe^- \rightarrow H_xWO_3 \quad (2)$$

The released electrons in Eq. (2) reduce the width of the depletion region in the oxide film, which changes the colour (from transparent to dark blue) and also the conductivity of the film, so that the resistance of the film decreases [28,50,51]. As the system is maintained at an elevated temperature, it is also possible that H_xWO_3 breaks down into reduced WO_3 producing H_2O vapour [7].

$$2H_xWO_3 \rightarrow xH_2O + 2WO_{3-\frac{x}{2}} \quad (3)$$

Upon exposing the sensors back to air (oxygen rich environment) the reduced oxide is restored to form WO_3 via:

$$WO_{3-\frac{x}{2}} + (\frac{x}{4})O_2 \rightarrow WO_3 \quad (4)$$

which allows the repeatability of the gas sensor.

It should be noticed here that the comparison of curves (a) and (b) in Fig. 5 shows that by repeating the gas sensing sequences the stability of the sensor gets better and its baseline gets more horizontal. This can be attributed to compensation of crystal defects as in oxygen vacancies, interstitial defects, dislocations, etc. It has been reported that thermal treatment increases the sensor performance. This improvement could be attributed to the transformation of WO_x to WO_3 [6]. However, in general these two curves prove the stability of the sensor. The WO_3 thin films exhibited large response magnitudes toward H_2 gas. The maximum response was measured to be 80% for 1% of H_2 at 250 °C. Considering curve (b) in Fig. 5, it was also found that the WO_3 based sensor produced repeatable responses of the same magnitudes for a H_2 exposure of the same concentration (i.e. 0.125% H_2). Fig. 6 shows the dynamic response and recovery of the WO_3 sensor towards 1% H_2 gas at different temperatures. As can be seen, the response magnitude and hence, the sensitivity of the sensor was increased with increasing operating temperature. Furthermore, it was observed that the response and recovery times decreased (which will be analysed and discussed in further detail later in this paper) with increasing operating temperature.

The curves presented in Fig. 7 show response vs. temperature for WO_3 sensor towards 0.06 (lowest tested concentration) and 1% (highest tested concentration) H_2 gas. At room temperature, the response magnitude is as low as 0 and 2% for 0.06 and 1% H_2 gas concentrations, respectively, however these values reach to about 48 and 80%, respectively, when the operating temperature is increased to 250 °C. For other H_2 concentrations including 0.125%, 0.25% and 0.5% at this temperature response values have been calculated to be about 56, 64 and 72, respectively. For comparison with this work, Kadir et al. have fabricated anodized nanoporous WO_3 Schottky contact structures for hydrogen and ethanol sensing. They have reported the gas responses of the fabricated sensor as 27.5%, 35.3%, 42.1%, 49.3% and 58.2%, in the presence of 0.06, 0.125, 0.25, 0.5 and 1% hydrogen gas, respectively, at the optimum temperature of 200 °C [7]. Despite the lower working temperature reported by the mentioned paper, it is observed that our nanostructured gas sensors have better response at same concentrations. Given that a simple operating temperature change results in such vast response magnitude improvements, it is postulated that further improvements

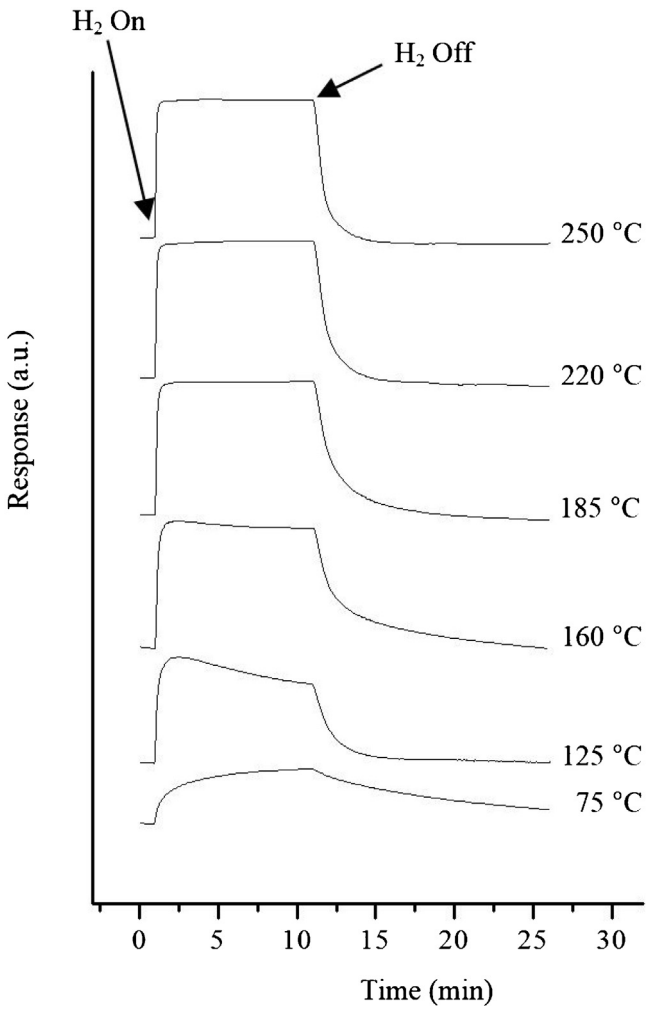

Fig. 6. Dynamic response and recovery of the WO_3 sensor towards 1% H_2 gas at different temperatures.

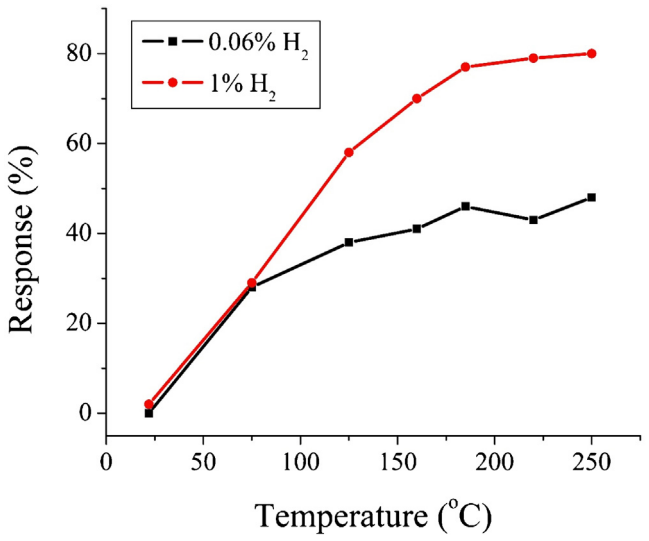

Fig. 7. Response vs. temperature for WO_3 sensor towards 0.06 and 1% H_2 gas concentrations.

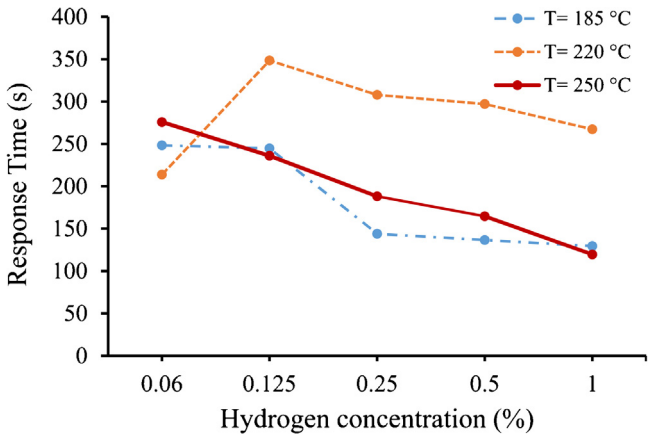

Fig. 8. Response time of the WO_3 sensor vs. H_2 concentration at different temperatures.

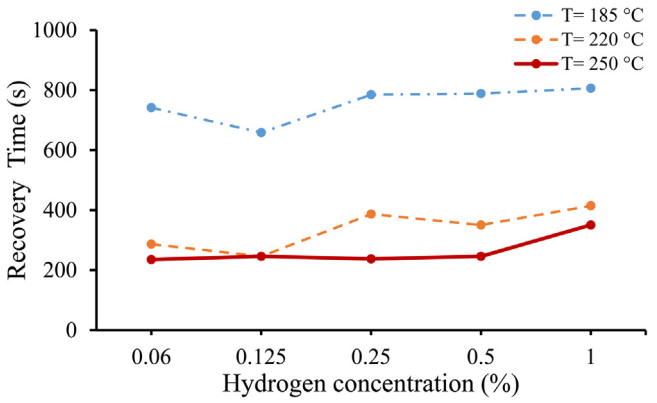

Fig. 9. Recovery time of the WO_3 sensor vs. H_2 concentration at different temperatures.

of sensing performance such as sensitivity, response and recovery times, selectivity and stability can be made by considering changes of other parameters in further works, including the use of different catalysts as well as the modification of WO_3 itself (i.e. through doping techniques).

The response time (τ_{res}) is defined as the time taken for the sensor resistance to reach 90% of its steady-state value and similarly, the recovery time (τ_{rec}) is defined as the time elapsed for 90% recovery of the total resistance change to be reached. Response and recovery times were obtained for the WO_3 sensors when exposed alternately to 0.06 (600 ppm), 0.125, 0.25, 0.5 and 1% of H_2 gas balanced in synthetic air. Figs. 8 and 9 show the analysis curves where response and recovery times are plotted against the tested H_2 concentrations, respectively, at three operating temperatures of 185, 220, and 250 °C. For lower temperatures, both the response and recovery times are significantly large. Furthermore, it can be observed that the response time is decreased while the recovery time is increased, when the amount of hydrogen content being tested is increased. Decreasing the response time can be attributed to the increasing amount of chemisorbed sites, due to the increase in the gas content. This has resulted in increasing the recovery time, as larger stoichiometry changes within the nanoplatelet films occur, which need longer recovery times to return to its initial (pre-exposure) condition [7]. The minimum of τ_{rec} is 235 s for 0.06% hydrogen concentration at 250 °C. Similarly, the minimum observed τ_{res} is 120 s for 1% hydrogen concentration at 250 °C. These minimum recorded values for τ_{rec} and τ_{res} at the tested concentrations confirm our proposed chemisorption mechanism.

4. Conclusion

High temperature anodized 2D WO_3 nanosheets based conductometric gas sensors were developed and their hydrogen sensing properties were investigated. The structure, morphology and gas sensing mechanism of WO_3 films were studied. High temperature anodized WO_3 thin films consisted of high aspect ratio nano-platelets with the width and the thickness in the range of 50–500 nm of 10–50 nm, respectively. The XRD analysis revealed that the WO_3 thin films are predominantly monoclinic crystal structure. The sensors were tested in a range of temperatures from 20 to 250 °C. This study showed maximum response of 80% for 1% of H_2 at 250 °C. The results underline that the developed H_2 gas sensors are worthy for further study and commercialization. The main advantage of the applied method in this paper is its simple and scalable rout for the fabrication of WO_3 nanosheets.

Acknowledgment

Mohammad Bagher Rahmani would like to acknowledge the Shahrood University of Technology for financial support. Authors acknowledge the RMIT microscopy and microanalysis facility (RMMF) and the technical staff therein for allowing and helping with the use of the microscopy and spectroscopy techniques used in this study.

References

[1] E. Comini, G. Faglia, G. Sberveglieri, Z.W. Pan, Z.L. Wang, Stable and highly sensitive gas sensors based on semiconducting oxide nanobelts, Appl. Phys. Lett. 81 (2002) 1869–1871.
[2] Y.M. Sabri, A.E. Kandjani, S.J. Ippolito, S.K. Bhargava, Ordered monolayer gold nano-urchin structures and their size induced control for high gas sensing performance, Sci. Rep. 6 (2016) 24625.
[3] S. Chen, Q. Zhang, J. Zhang, J. Gu, L. Zhang, Synthesis of two conjugated polymers as TNT chemosensor materials, Sens. Actuators B 149 (2010) 155–160.
[4] G. Korotcenkov, Metal oxides for solid-state gas sensors: what determines our choice? Mater. Sci. Eng.: B 139 (2007) 1–23.
[5] A. Zoshki, M.B. Rahmani, F. Masdarolomoor, S.H. Pilehrood, Room temperature gas sensing properties of polyaniline/ZnO nanocomposite thin films, J. Nanoelectron. Optoelectron. 12 (2017) 465–471.
[6] Y.-A. Lee, S.S. Kalanur, G. Shim, J. Park, H. Seo, Highly sensitive gasochromic H_2 sensing by nano-columnar WO_3-Pd films with surface moisture, Sens. Actuators B 238 (2017) 111–119.
[7] R. Ab Kadir, W. Zhang, Y. Wang, J.Z. Ou, W. Wlodarski, A.P. O'Mullane, et al., Anodized nanoporous WO3 Schottky contact structures for hydrogen and ethanol sensing, J. Mater. Chem. A 3 (2015) 7994–8001.
[8] X. Chen, Y. Zhou, Q. Liu, Z. Li, J. Liu, Z. Zou, Ultrathin, single-Crystal WO_3 nanosheets by two-dimensional oriented attachment toward enhanced photocatalystic reduction of CO_2 into hydrocarbon fuels under visible light, ACS Appl. Mater. Interfaces 4 (2012) 3372–3377.
[9] M.B. Rahmani, M. Breedon, D. Lau, J.L. Campbell, A. Moafi, D.G. McCulloch, et al., Gas sensing properties of interconnected ZnO nanowires, Sens. Lett. 9 (2011) 929–935.
[10] Z.L. Wang, ZnO nanowire and nanobelt platform for nanotechnology, Mater. Sci. Eng. R-Rep. 64 (2009) 33–71.
[11] S. Zhuiykov, E. Kats, B. Carey, S. Balendhran, Proton intercalated two-dimensional WO_3 nano-flakes with enhanced charge-carrier mobility at room temperature, Nanoscale 6 (2014) 15029–15036.
[12] S. Balendhran, S. Walia, M. Alsaif, E.P. Nguyen, J.Z. Ou, S. Zhuiykov, et al., Field effect biosensing platform based on 2D α-MoO_3, ACS Nano 7 (2013) 9753–9760.
[13] M.M.Y.A. Alsaif, M.R. Field, T. Daeneke, A.F. Chrimes, W. Zhang, B.J. Carey, et al., Exfoliation solvent dependent plasmon resonances in two-Dimensional sub-Stoichiometric molybdenum oxide nanoflakes, ACS Appl. Mater. Interfaces 8 (2016) 3482–3493.
[14] M.M.Y.A. Alsaif, A.F. Chrimes, T. Daeneke, S. Balendhran, D.O. Bellisario, Y. Son, et al., High-Performance field effect transistors using electronic inks of 2D molybdenum oxide nanoflakes, Adv. Funct. Mater. 26 (2016) 91–100.
[15] S.B. Upadhyay, R.K. Mishra, P.P. Sahay, Structural and alcohol response characteristics of Sn-doped WO3 nanosheets, Sens. Actuators B 193 (2014) 19–27.
[16] N. Yamazoe, New approaches for improving semiconductor gas sensors, Sens. Actuators B-Chem. 5 (1991) 7–19.
[17] A.Z. Sadek, H.D. Zheng, K. Latham, W. Wlodarski, K. Kalantar-Zadeh, Anodization of Ti thin film deposited on ITO, Langmuir 25 (2009) 509–514.
[18] H.D. Zheng, A.Z. Sadek, K. Latham, K. Kalantar-Zadeh, Nanoporous WO3 from anodized RF sputtered tungsten thin films, Electrochem. Commun. 11 (2009) 768–771.
[19] M. Breedon, M.B. Rahmani, S.-H. Keshmiri, W. Wlodarski, K. Kalantar-zadeh, Aqueous synthesis of interconnected ZnO nanowires using spray pyrolysis deposited seed layers, Mater. Lett. 64 (2010) 291–294.
[20] M.B. Rahmani, S.H. Keshmiri, J. Yu, A.Z. Sadek, L. Al-Mashat, A. Moafi, et al., Gas sensing properties of thermally evaporated lamellar MoO3, Sens. Actuators B 145 (2010) 13–19.
[21] M.B. Rahmani, S.H. Keshmiri, M. Shafiei, K. Latham, W. Wlodarski, J. du Plessis, et al., Transition from n- to p-Type of spray pyrolysis deposited Cu doped ZnO thin films for NO_2 sensing, Sens. Lett. 7 (2009) 621–628.
[22] L.F. Dong, Z.L. Cui, Z.K. Zhang, Gas sensing properties of nano-ZnO prepared by arc plasma method, Nanostruct. Mater. 8 (1997) 815–823.
[23] S.H. Mousavi-Zadeh, M.B. Rahmani, Thin film growth and Zn doping of h-MoO_3 hexagonal rods by hydrothermal technique, Mod. Phys. Lett. B (2016) 1650424.
[24] V. Kruefu, A. Wisitsoraat, A. Tuantranont, S. Phanichphant, Ultra-sensitive H2S sensors based on hydrothermal/impregnation-made Ru-functionalized WO3 nanorods, Sens. Actuators B 215 (2015) 630–636.
[25] R.G. Palgrave, I.P. Parkin, Aerosol assisted chemical vapour deposition of photochromic tungsten oxide and doped tungsten oxide thin films, J. Mater. Chem. 14 (2004) 2864–2867.
[26] C. Cantalini, L. Lozzi, A. Passacantando, S. Santucci, The comparative effect of two different annealing temperatures and times on the sensitivity and long-term stability of WO_3 thin films for detecting NO_2, IEEE Sens. J. 3 (2003) 171–179.
[27] G. Sberveglieri, L. Depero, S. Groppelli, P. Nelli, WO_3 sputtered thin-films for NO_X monitoring, Sens. Actuators B-Chem. 26 (1995) 89–92.
[28] M.H. Yaacob, M. Breedon, K. Kalantar-Zadeh, W. Wlodarski, Absorption spectral response of nanotextured WO3 thin films with Pt catalyst towards H-2, Sens. Actuators B-Chem. 137 (2009) 115–120.
[29] J. Guerin, K. Aguir, M. Bendahan, C. Lambert-Mauriat, Thermal modelling of a WO_3 ozone sensor response, Sens. Actuators B-Chem. 104 (2005) 289–293.
[30] K.J. Lethy, D. Beena, R. Vinod Kumar, V.P. Mahadevan Pillai, V. Ganesan, V. Sathe, Structural, optical and morphological studies on laser ablated nanostructured WO_3 thin films, Appl. Surf. Sci. 254 (2008) 2369–2376.
[31] S. Cao, C. Zhao, T. Han, L. Peng, Hydrothermal synthesis, characterization and gas sensing properties of the WO3 nanofibers, Mater. Lett. 169 (2016) 17–20.
[32] C. Santato, M. Odziemkowski, M. Ulmann, J. Augustynski, Crystallographically oriented mesoporous WO_3 films: synthesis, characterization, and applications, J. Am. Chem. Soc. 123 (2001) 10639–10649.
[33] M. Breedon, P. Spizzirri, M. Taylor, J. du Plessis, D. McCulloch, J. Zhu, et al., Synthesis of nanostructured tungsten oxide thin films: a simple, controllable, inexpensive, aqueous sol-gel method, Cryst. Growth Des. 10 (2009) 430–439.
[34] N. Mukherjee, M. Paulose, O.K. Varghese, G.K. Mor, C.A. Grimes, Fabrication of nanoporous tungsten oxide by galvanostatic anodization, J. Mater. Res. 18 (2003) 2296–2299.
[35] K. Kalantar-zadeh, A.Z. Sadek, H. Zheng, V. Bansal, S.K. Bhargava, W. Wlodarski, et al., Nanostructured WO3 films using high temperature anodization, Sens. Actuators B 142 (2009) 230–235.
[36] H. Tsuchiya, J.M. Macak, I. Sieber, L. Taveira, A. Ghicov, K. Sirotna, et al., Self-organized porous WO3 formed in NaF electrolytes, Electrochem. Commun. 7 (2005) 295–298.
[37] R. Hahn, J.M. Macak, P. Schmuki, Rapid anodic growth of TiO2 and WO3 nanotubes in fluoride free electrolytes, Electrochem. Commun. 9 (2007) 947–952.
[38] A. Boudiba, P. Roussel, C. Zhang, M.-G. Olivier, R. Snyders, M. Debliquy, Sensing mechanism of hydrogen sensors based on palladium-loaded tungsten oxide (Pd–WO_3), Sens. Actuators B 187 (2013) 84–93.
[39] W. Meng, L. Dai, J. Zhu, Y. Li, W. Meng, H. Zhou, et al., A novel mixed potential NH3 sensor based on TiO2@WO3 core?shell composite sensing electrode, Electrochim. Acta 193 (2016) 302–310.
[40] E. Llobet, G. Molas, P. Molinas, J. Calderer, X. Vilanova, J. Brezmes, et al., Fabrication of highly selective tungsten oxide ammonia sensors, J. Electrochem. Soc. 147 (2000) 776–779.
[41] C.S. Rout, M. Hegde, C.N.R. Rao, H2S sensors based on tungsten oxide nanostructures, Sens. Actuators B-Chem. 128 (2008) 488–493.
[42] Y.S. Kim, Thermal treatment effects on the material and gas-sensing properties of room-temperature tungsten oxide nanorod sensors, Sens. Actuators B-Chem. 137 (2009) 297–304.
[43] O.K. Varghese, D.W. Gong, M. Paulose, K.G. Ong, C.A. Grimes, Hydrogen sensing using titania nanotubes, Sens. Actuators B-Chem. 93 (2003) 338–344.
[44] P.B. Bennett, R.E. Marquis, Basic and Applied High Pressure Biology, University of Rochester Press, 1994.
[45] T. Nishide, F. Mizukami, Crystal structures and optical properties of tungsten oxide films prepared by a complexing-agent-assisted sol-gel process, Thin Solid Films 259 (1995) 212–217.
[46] Y.P. Xie, G. Liu, L. Yin, H.-M. Cheng, Crystal facet-dependent photocatalytic oxidation and reduction reactivity of monoclinic WO_3 for solar energy conversion, J. Mater. Chem. 22 (2012) 6746–6751.
[47] C.V. Ramana, S. Utsunomiya, R.C. Ewing, C.M. Julien, U. Becker, Electron microscopy investigation of structural transformations in tungsten oxide (WO_3) thin films, Physica Satus Solidi (A) 202 (2005) R108–R110.

[48] W. Yu-De, C. Zhan-Xian, L. Yan-Feng, Z. Zhen-Lai, W. Xing-Hui, Electrical and gas-sensing properties of WO3 semiconductor material, Solid-State Electron. 45 (2001) 639–644.
[49] T. Hübert, L. Boon-Brett, G. Black, U. Banach, Hydrogen sensors–a review, Sens. Actuators B 157 (2011) 329–352.
[50] J.Z. Ou, S. Balendhran, M.R. Field, D.G. McCulloch, A.S. Zoolfakar, R.A. Rani, et al., The anodized crystalline WO3 nanoporous network with enhanced electrochromic properties, Nanoscale 4 (2012) 5980–5988.
[51] J.Z. Ou, M.H. Yaacob, M. Breedon, H.D. Zheng, J.L. Campbell, K. Latham, et al., In situ Raman spectroscopy of H2 interaction with WO3 films, Phys. Chem. Chem. Phys. 13 (1) (2011) 7330–7339.

Biographies

Mohammad Bagher Rahmani is currently an assistant professor of physics at the Shahrood University of Technology. He received his BSc in physics from Shahid Bahonar University of Kerman, Iran (2000), and MSc and PhD in solid state physics from Ferdowsi University of Mashhad, Iran (2004 and 2010, respectively). He spent his PhD research leave at RMIT (2009). His research interests include chemical gas sensors, nanostructured transparent semiconducting oxides, solar cells, and conducting polymers.

Mohd Hanif Yaacob received his Bachelor of Engineering (Electronic Computer Systems), Master of Science (Communication and Network Engineering) and PhD (Electrical and Computer Engineering) from Salford University, UK (1999), Universiti Putra Malaysia, Malaysia (2002) and RMIT University, Australia (2012), respectively. Currently, he is a lecturer at the Department of Computer & Communication Systems Engineering, Universiti Putra Malaysia. His research interests are optical gas sensors, optical communication systems and nanotechnology.

Ylias Mohammad Sabri received his a chemical engineer degree (2003) and PhD (Applied Chemistry, 2010) from RMIT University. He is currently senior research fellow at RMIT University working in the areas of transducer based gas sensors, optical sensors, biosensors, nanomaterials synthesis, catalysis and photocatalysis